Palaeogeography, Palaeoclimatology, Palaeoecology xxx (2008) xxx–xxx

Contents lists available at ScienceDirect

Palaeogeography, Palaeoclimatology, Palaeoecology

journal homepage: www.elsevier.com/locate/palaeo

Present-day South American climate

René D. Garreaud [a,*], Mathias Vuille [b], Rosa Compagnucci [c], José Marengo [d]

[a] Department of Geophysics, Universidad de Chile, Blanco Encalada 2002, Santiago, Chile
[b] Department of Earth and Atmospheric Sciences, University at Albany, State University of New York, Albany NY, USA
[c] Departamento de Ciencias de la Atmósfera y los Océanos, Facultad de Ciencias Exactas y Naturales, Universidad de Buenos Aires, Buenos Aires, Argentina
[d] Centro de Previsão de Tempo e Estudos Climáticos/INPE, Cachoeira Paulista, Sao Paulo, Brazil

ARTICLE INFO

Article history:
Received 25 April 2007
Accepted 13 October 2007
Available online xxxx

Keywords:
Climate
Atmospheric circulation
Precipitation
Climate variability
South America

ABSTRACT

This paper documents the main features of the climate and climate variability over South America, on the basis of instrumental observations gathered during the 20th Century. It should provide a modern reference framework for paleoclimate research in South America, targeting high-resolution proxies over the past few centuries. Several datasets suitable for present-day climate research are first described, highlighting their advantages as well as their limitations. We then provide a basic physical understanding of the mean annual cycle of the precipitation and atmospheric circulation over the continent and the adjacent oceans. In particular, the diversity of precipitation, temperature and wind patterns is interpreted in terms of the long meridional extent of the continent and the disruption of the large-scale circulation caused by the Andes cordillera, the contrasting oceanic boundary conditions and the landmass distribution. Similarly, the intensity and timing of the interannual and interdecadal climatic fluctuations exhibit considerable geographical dependence, as some regions are more influenced by large-scale phenomena rooted in the tropical oceans while others are more influenced by high-latitude phenomena. The impact of these large-scale phenomena over South America is documented by a regression analysis between selected atmospheric indices and the precipitation and temperature fields. We have included a discussion on the seasonality and long-term stability of such impacts, and complemented our general description by an updated review of the literature on climate variability over specific regions.

1. Introduction

Owing to its considerable meridional extension and prominent orography, South America exhibits diverse patterns of weather and climate, including tropical, subtropical and extratropical features. The Andes cordillera runs continuously near the west coast of the continent with elevations in excess of 4 km from north of the equator to the south of 40°S (farther south it still rises over 2 km in many places) and therefore represents a formidable obstacle for the tropospheric flow. The Andes not only act as a climatic wall with dry conditions to the west and moist conditions to the east at tropical/subtropical latitudes (the pattern reverses in midlatitudes) but they also foster tropical–extratropical interactions, especially along their eastern side. The Brazilian plateau also tends to block the low-level circulation over subtropical South America, and the large area of continental landmass at low latitudes (10°N–25°S) is conducive to the development of intense convective storms that support the world's largest rain forest in the Amazon basin. The variability of the South American climate (i.e., interannual and interdecadal changes) results from the superposition of several large-scale phenomena. The El Niño Southern Oscillation (ENSO) phenomenon is rooted in the ocean-atmosphere system in the tropical Pacific, and thus it has a strong, direct effect over coastal Ecuador, Perú and northern Chile, as well as an indirect effect (through atmospheric teleconnections) over much of subtropical South America extending also to high-latitudes. Similarly, the sea surface temperature (SST) meridional gradient over the tropical Atlantic has a profound impact on the climate and weather of eastern South America. Droughts in Amazonia and North-eastern Brazil have been linked to anomalously warm surface waters in the tropical North Atlantic. High-latitude forcing, such as by the Antarctic Oscillation (AAO) and the North Atlantic Oscillation (NAO), seems to also play a role in climate variability over South America.

The main features of the atmospheric circulation over the Southern Hemisphere were presented by van Loon (1972) in the first Southern Hemisphere Meteorological Monograph. A detailed survey of regional climate elements on a country-by-country basis is presented by Schwerdtfeger and Landsberg (1976). Later on, Satyamurty et al. (1998) review the mean continental-scale circulation, the most frequent synoptic-scale (weather) disturbances, and teleconnections with planetary-scale phenomena (e.g., ENSO). The work of Satyamurty et al. (1998) focuses on tropical/subtropical South America and includes a discussion on the climatic impacts of Amazonian deforestation.

* Corresponding author. Tel.: +56 2 9784310.
E-mail address: rgarreau@dgf.uchile.cl (R.D. Garreaud).

0031-0182/$ – see front matter © 2008 Elsevier B.V. All rights reserved.
doi:10.1016/j.palaeo.2007.10.032

Garreaud and Aceituno (2007) include similar topics to those covered by Satyamurty et al. (1998), but here the emphasis is placed on the subtropical/extratropical part of the continent. In the last decade, climatologists have begun to describe the climate of the northern and central part of the continent as monsoon-like; an updated review of the so-called South American Monsoon System (SAMS) is presented by Vera et al. (2006). Reviews of the climate of the Amazon basin have been detailed by Marengo (2004) and Marengo and Nobre (2001), while a comprehensive study of the climate in the La Plata Basin has been produced by Barros et al. (2000). Similarly, a review paper on the climate of the Altiplano (central Andes) is provided by Garreaud et al. (2003).

The aim of this paper is to review the climate and climate variability over South America, with particular emphasis on the year-to-year and longer fluctuations of rainfall and temperature at continental- and regional-scales. It should provide a modern reference framework for paleoclimate research in South America, targeting high-resolution proxies (e.g., tree-rings, ice cores and speleothems) over the past few centuries. Our description is facilitated by a relatively dense network of surface and upper-air instrumental observations, but its temporal scope is mostly limited to the second half of the 20th century (see details in Section 2). For the sake of simplicity (but somewhat arbitrarily) tropical/subtropical and extratropical mean features are described separately (Section 3). In Section 4, we describe how the leading modes of global atmospheric variability (e.g., ENSO, AAO) affect the regional climate, including the seasonality and long-term stability of such forcings. In some regions, however, climate variability might be influenced by several modes acting simultaneously. Our "top-down" analysis is therefore complementary with the "bottom-up" approach (followed in many other studies) in which climate indices of specific regions (e.g., the Altiplano) are regressed upon global fields (e.g., SST). In the latter case, the results portray the large-scale circulation patterns which most directly modulate regional variability; however, these patterns aren't necessarily an actual mode of the atmospheric circulation.

2. Datasets

In this section we provide an overview of different datasets suitable for climate research, including conventional station data, gridded products and atmospheric reanalysis. We focus on those datasets easily available for the research community, some of which are used in this paper. Table 1 presents the main features of these products.

Near-surface weather stations, with their suite of meteorological instruments, provide real-time observations for many applications ranging from agriculture to forecasting, and their historical records are fundamental for climate research. Networks of such stations are operated at local and country levels by national weather services (NWSs) and other institutions (Fig. 1a). There are, however, practical problems in using these data for climate studies, including difficulties in data access, non-digitized records, inhomogeneities, and presence of data errors. Therefore, several efforts have aimed at producing regional and global, long-term, quality-controlled, datasets of instrumental observations suitable for climate research. Of particular relevance is the Global Historical Climatology Network (GHCN), comprised of century-long, worldwide surface observations (~7000 stations) of temperature and precipitation on a monthly basis. Currently, GHCN Version-2 data (Peterson and Vose, 1997) is regularly updated and freely available from the United States (US) National Climatic Data Center (NCDC) web site. Fig. 1c and d shows the distribution of GHCN stations over South America with an indication of their record length. When considering all the GHCN stations the coverage is very complete and the station density is high, especially for precipitation. However, there are only 51 (20) precipitation (mean temperature) stations whose records extend through the 20th century and have more than 80% of the data for that period, mostly located along the coastlines.

Near century-long, interpolated gridded datasets are also produced by several centres and extensively used in climate studies, especially in those seeking to find spatial patterns of variability. These products are typically on a regular latitude–longitude mesh with horizontal grid-spacing of a few hundred kilometers, and they have monthly resolution. For temperature, each grid-box value is the average of all available station anomalies (departures from the station climatology) within the box. Using anomalies (instead of the full values) reduces the problem of interpolating station data over complex terrain. For precipitation, the gridding scheme uses more sophisticated methods (e.g., Thiessen polygon, topographic weights). When using these gridded datasets it is important to keep in mind that over remote areas, the gridded values might be derived from few stations (perhaps just one, or none at all), hampering their accurate

Table 1
Main features of datasets commonly used in climate studies

Dataset	Key references	Input data — variables	Spatial resolution — coverage	Time span — time resolution
Station	Peterson and Vose (1997)	Sfc. Obs	N/A	1850(*)–present
GHCN		Precip and SAT	Land only	Daily and monthly
Gridded	Peterson and Vose (1997)	Sfc. Obs	5°×5° lat–lon	1900–present
GHCN		Precip and SAT	Land only	Monthly
Gridded	New et al. (2000)	Sfc. Obs	0.5°×0.5° lat–lon	1900–present
UEA-CRU		Precip and SAT	Land only	Monthly
Gridded	Mitchell and Jones (2005)	Sfc. Obs	0.5°×0.5° lat–lon	1901–present
UEA-CRU05		Precip and SAT	Land only	Monthly
Gridded	Legates and Willmont (1999a,b)	Sfc. Obs	0.5°×0.5° lat–lon	1950–1999
U. Delaware		Precip and SAT	Land only	monthly
Gridded	Liebmann and Allured (2005)	Sfc. Obs	1°×1° lat–lon	1940–2006
SAM-CDC data		Precip	South America	Daily and monthly
Gridded	Xie and Arkin (1997)	Sfc. Obs.; Sat. data	2.5°×2.5° lat–lon	1979–present
CMAP		Precip	Global	Pentad and monthly
Gridded	Adler et al. (2003)	Sfc. Obs.; Sat. data	2.5°×2.5° lat–lon	1979–present
GPCP		Precip	Global	Monthly
NCEP-NCAR	Kalnay et al. (1996)	Sfc. Obs.; UA Obs; Sat. data	2.5°×2.5° lat–lon, 17 vertical levels	1948–present
Reanalysis (NNR)	Kistler et al. (2001)	Pressure, temp., winds, etc.	Global	6 h, daily, monthly
ECMWF	Uppala et al. (2005)	Sfc. Obs., UA Obs, Sat. data	2.5°×2.5° lat–lon, 17 vertical levels	1948–present
Reanalysis (ERA-40)		Pressure, temp., winds, etc.	Global	6 h, daily, monthly

Notes:
Input data refer to the types of data used to construct the database: Sfc. Obs. = observations taken at near-surface meteorological stations; Sat. data: satellite estimates of several variables (most commonly precipitation); UA Obs: upper-air observations most commonly taken from radiosondes.
Variables refer to the meteorological parameter included in each dataset: Precip = precipitation; SAT = Surface air temperature; temp = Air temperature at various levels.

Please cite this article as: Garreaud, R.D., et al., Present-day South American climate, Paleogeogr. Palaeoclimatol. Palaeoecol. (2008), doi:10.1016/j.palaeo.2007.10.032

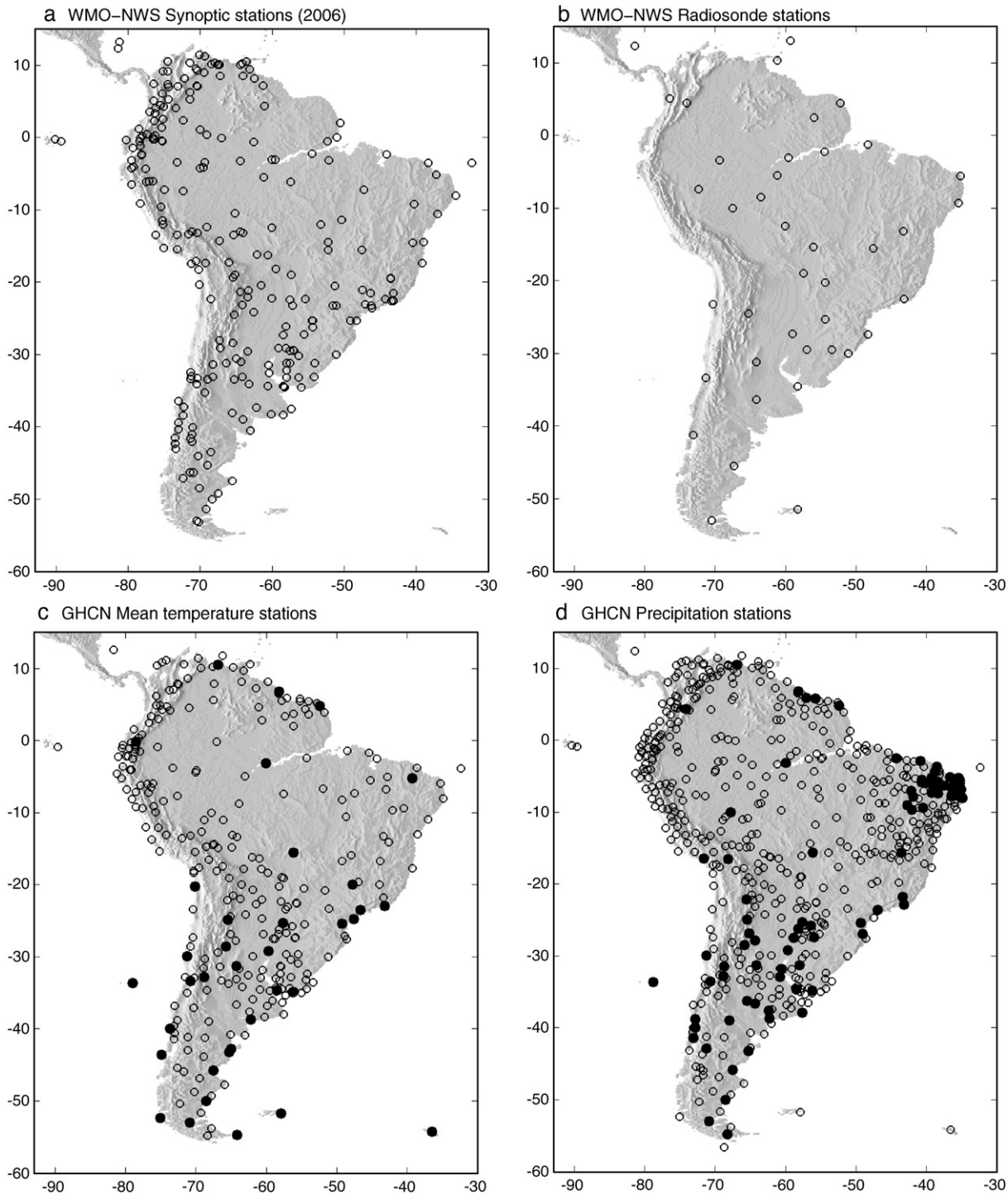

Fig. 1. (a) Map of surface stations reporting synoptic observations (surface pressure, air temperature, present weather, etc., every 6 or 12 h) during the year 2006. These stations are operated by National Weather Services (NWS) that form part of the World Meteorological Organization. (b) As (a) but radiosonde stations (thus providing upper-air data). (c) Map of GHCN mean temperature stations. Open circles indicate all the stations that have operated in South America regardless of its record length and continuity; filled circles indicate those stations that began to operate in 1901 (or before) and have more than 80% of the data during the 20th century. (d) As (c) but for GHCN precipitation stations.

representation of the real climatic conditions. Here we use global, high-resolution grids (0.5°×0.5° lat–lon) from 1959–1999, produced by the Center for Climatic Research, University of Delaware (Legates and Willmont, 1990a,b). Fully global (land and ocean) gridded precipitation data is only available since the late 70s, when satellite derived rainfall estimates became available. The most popular products in this category are the Climate Prediction Center Merged Analysis of Precipitation (CMAP; Xie and Arkin, 1997) and the Global Precipitation Climatology Project (GPCP; Adler et al., 2003).

Atmospheric near-surface variables have the most direct impact upon other earth-systems (e.g., biosphere) and are commonly targeted in paleoclimate reconstructions, but they are a reflection of meteorological phenomena that are inherently three-dimensional. To describe them, vertical profiles of wind, temperature, pressure and humidity between the surface and the upper troposphere (generically termed upper-air data) are primarily obtained from radiosonde measurements, and more recently from satellite- and surface-based remote sensing instruments. Radiosondes are launched once or twice daily (00:00 and 12:00 UTC) from a

Please cite this article as: Garreaud, R.D., et al., Present-day South American climate, Paleogeogr. Palaeoclimatol. Palaeoecol. (2008), doi:10.1016/j.palaeo.2007.10.032

network of stations operated by NWSs. The global radiosonde network began to operate in 1958, and owing to the high cost of these instruments it is much sparser than the surface meteorological network (Fig. 1b).

Surface, radiosonde and satellite data are transmitted in real-time by NWSs and assimilated into three-dimensional matrices (lat–long-height) that seek to represent the state of the atmosphere at a given time. These so-called "meteorological analyses" are constructed operationally four-times daily since the early 60s, mainly in support of weather forecast. Furthermore, a few meteorological centres have undertaken "reanalysis projects", in which the resulting global, gridded fields are produced using a frozen assimilation system and an enhanced observational database. Given their temporal continuity, global coverage and physical consistency, reanalysis data is widely used in climate studies (e.g., to describe interannual variability). Nevertheless, two caveats are in order. First, measured precipitation is not assimilated in the reanalysis, and therefore the reanalysis precipitation fields, while consistent with the atmospheric circulation, are model-dependent. Thus, for climate studies dealing with precipitation it is better to use observational datasets. Secondly, reanalysis still may have spurious (non-physical) trends due to the change in time of the number and type of data assimilated into them. This problem is particularly marked in the Southern Hemisphere mid- and high-latitudes (e.g., Marshall, 2003), so the ability of the reanalysis to capture decadal variability and secular trends is marginal at best. It has been suggested that the quality of the reanalysis data over the SH has improved after the late seventies due to the availability of global satellite data (e.g., Kalnay et al., 1996).

Since its release in the mid 90s, the National Centers for Environmental Prediction–National Center for Atmospheric Research reanalysis (NNR, Kalnay et al., 1996) has been extensively used in climate research. The NNR data are available for the period been 1948 to the present on a 2.5°×2.5° lat–long global grid. The European Centre for Medium-range Weather Forecast (ECMWF) also produced reanalysis data that cover the 40-year period 1957–2002 (the so-called ERA-40 product; Uppala et al., 2005) with similar resolution as NNR. There are many studies comparing NNR and ERA-40 (e.g., Wang et al., 2006); both data sets are in general agreement and it is not possible to conclude that one product supersedes the other. In this paper we use NCEP-NCAR reanalysis.

3. Mean fields and annual cycles

3.1. Tropical and subtropical features

Fig. 2a and b shows the long-term mean precipitation for July and January, superimposed upon the corresponding low-level (925 hPa, about 1 km above sea level [ASL]) winds. The precipitation field exhibits several maxima: along a rather narrow, east–west oriented band over the tropical oceans called the Intertropical Convergence Zone (ITCZ), in a broad area over the continent

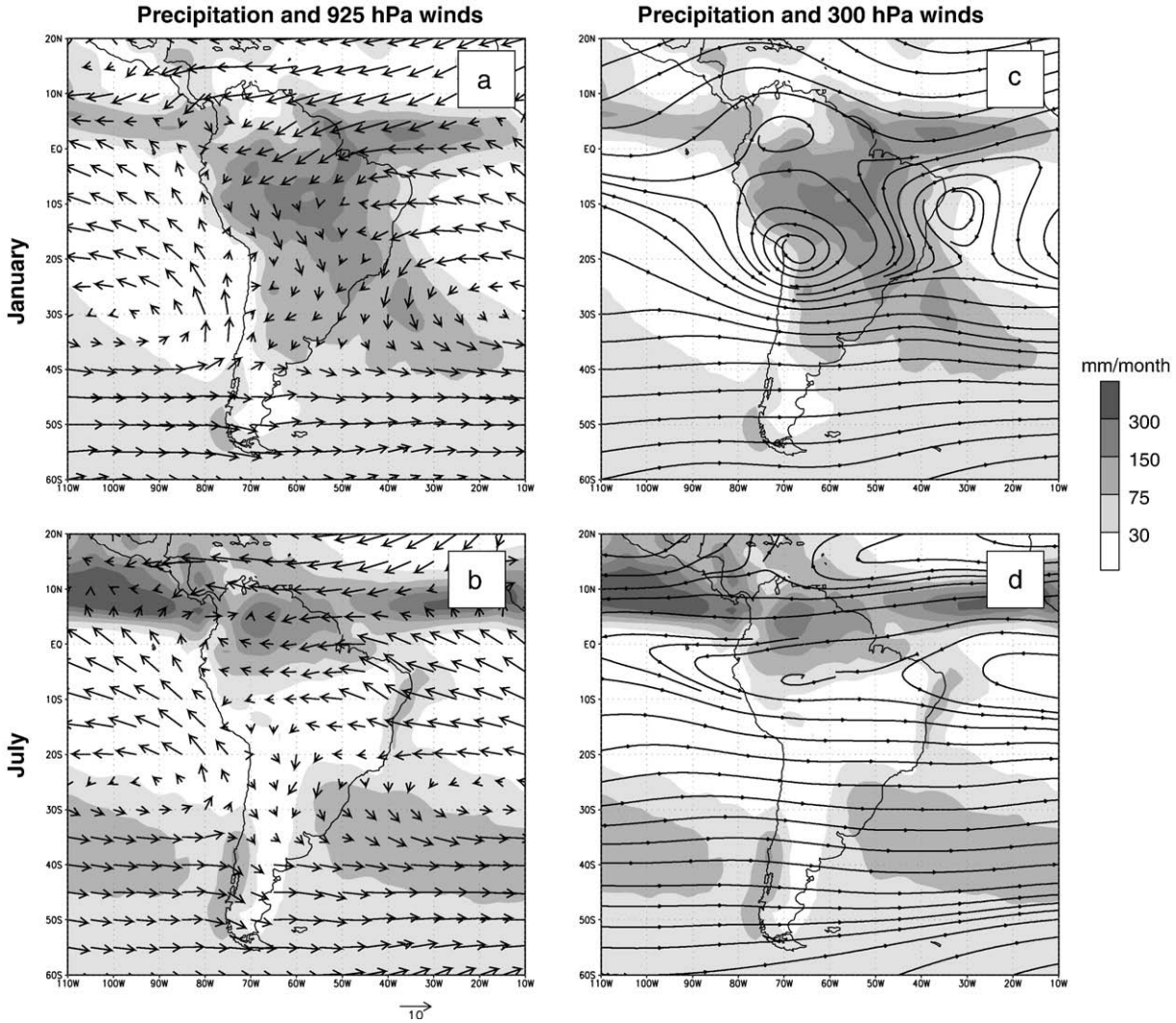

Fig. 2. Left panels: long-term mean CMAP precipitation (shaded — scale at right) and 925 hPa wind vectors (arrows — scale at bottom) for (a) January and (b) July. Right panels: long-term mean precipitation (shaded — scale at right) and streamlines at 300 hPa (streamlines) for (c) January and (d) July.

Please cite this article as: Garreaud, R.D., et al., Present-day South American climate, Paleogeogr. Palaeoclimatol. Palaeoecol. (2008), doi:10.1016/j.palaeo.2007.10.032

(particularly well developed during austral summer), and along broad bands over the extratropical oceans. Let us describe these features in some details.

The ITCZ corresponds to the belt of minimum pressure (not shown) and intense low-level convergence of the trade winds over the equatorial oceans. Precipitation over the ITCZ is mostly of convective nature, produced by deep cumulus–nimbus. Due to atmosphere-ocean feedbacks instigated by the orientation of the coastline (Mitchell and Wallace, 1992), the ITCZ over the eastern Pacific resides to the north of 5°N year round (the so-called northerly bias), except during intense El Niño events (Horel and Cornejo-Garrido, 1986). Over the tropical Atlantic sector the ITCZ reaches the equator, producing the rainy season of northeast Brazil. In contrast to the copious precipitation near the ITCZ, rainfall is nearly absent over broad areas of the subtropical oceans due to the large-scale mid-tropospheric subsidence. The subsidence also maintains semi-permanent high-pressure cells, apparent in Fig. 2a and b by the anti-cyclonic (counter clockwise) low-level flow around their centres at about 30°S. The subsidence over the subtropical SE Pacific and SW Atlantic is most intense in austral winter but encompass a larger meridional extent in austral summer (e.g., Dima and Wallace, 2003). The convergence of the moisture-laden trade winds, the intense ascent and convection over the ITCZ, the poleward divergence near the tropopause, and the more gentle descent of dry air over the subtropics form a closed loop known as the Hadley circulation.

Consistent with the low thermal inertia of the land, tropical/subtropical rainfall over the continent experiences a pronounced seasonal cycle (e.g., Horel et al., 1989; Fu et al., 1998; Marengo et al., 2001). During the austral winter, the maximum continental rainfall is located to the north of the equator, almost in line with the oceanic ITCZ, while the central part of the continent (including southern Amazonia) experiences its dry season. By the end of October there is a rapid southward shift of the convection, so that during the austral summer a broad area of heavy precipitation extends from the southern half of the Amazon Basin to northern Argentina. During austral fall, the precipitation maximum returns gradually to northern South America. Such migration has led many scientists to describe the climate of the central part of South America as Monsoon-like (Zhou and Lau, 1998; Vera et al., 2006). The climate is not fully monsoonal, however, because the low-level winds never reverse their direction. Throughout the year the trade winds over the Atlantic blow toward the continent (albeit with different angles) where the pressure is lower than over the ocean.

During austral summer a very deep continental low forms over the Chaco region (~25°S; Seluchi et al., 2003) and forces the easterly winds over the Amazon basin to turn southward, being channelled between the eastern slope of the Andes and the Brazilian Plateau. The northerly flow often exhibits a low-level jet structure (Saulo et al., 2000; Marengo et al., 2004), with its core at about 1 km ASL, transporting large amounts of moisture that feeds summertime convective storms over the subtropical plains as far south as 35°S. Also during summer, the latent heat released by the Cumulus convection over the Amazon Basin leads to the formation of an upper-level high-pressure cell (Lenters and Cook, 1997). The so-called Bolivian High is persistent enough as to appear in the monthly and seasonal averages at the 200 hPa level (about 12 km ASL; Fig. 2c) and it is accompanied by a cyclonic circulation downstream over the northeast coast of Brazil (Virji, 1981; Chen et al., 1999). In

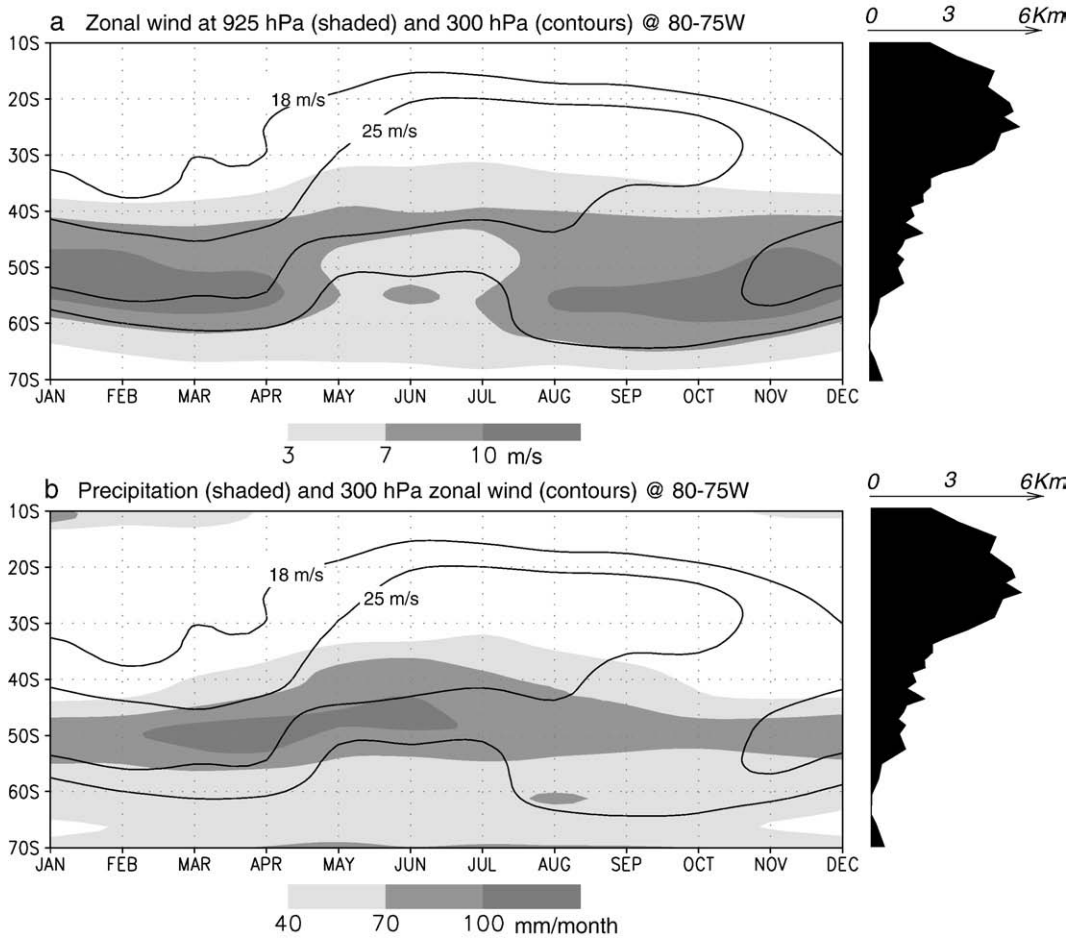

Fig. 3. (a) Latitude–time cross section of the long-term-mean 300 hPa (contours) and 925 hPa (shaded — scale at bottom) zonal wind speed. Both variables were averaged between 80° and 75°W. Black area at the right schematize the topography of the west half of South America (dominated by the Andes cordillera). (b) As in (a) but the shaded field is long-term-mean CMAP precipitation.

Please cite this article as: Garreaud, R.D., et al., Present-day South American climate, Paleogeogr. Palaeoclimatol. Palaeoecol. (2008), doi:10.1016/j.palaeo.2007.10.032

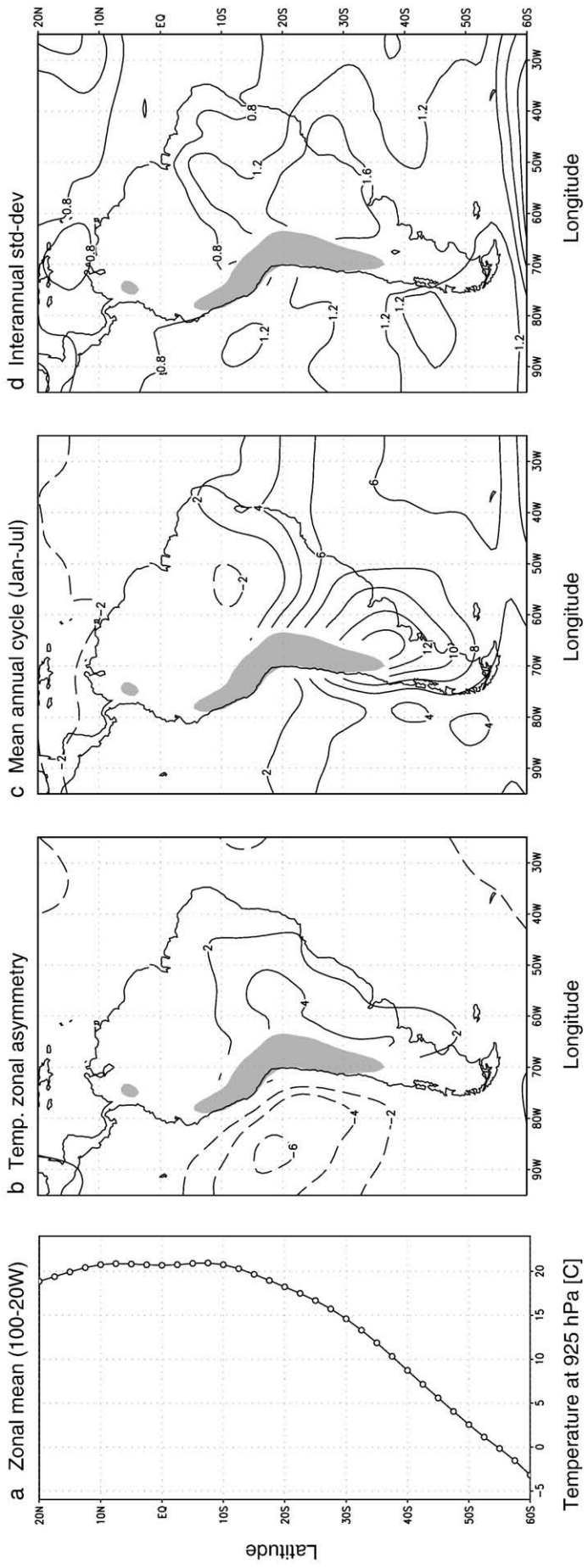

Fig. 4. (a) Annual mean of the 925 hPa air temperature averaged between 100°W and 20°W ([*T*]). (b) Zonally asymmetric component of the annual mean 925 hPa air temperature ([*T*] was subtracted from the annual mean field). Contour interval is 2 °C, negative values in dashed line, and the zero contour is omitted. (c) January minus July mean air temperature at 925 hPa. Contour interval is 2 °C, negative values in dashed line, and the zero contour is omitted. (d) Interannual standard deviation of the annual mean temperature, contoured every 0.4 °C.

Please cite this article as: Garreaud, R.D., et al., Present-day South American climate, Paleogeogr. Palaeoclimatol. Palaeoecol. (2008), doi:10.1016/j.palaeo.2007.10.032

connection with the Bolivian High, mid- and upper-level easterly winds appear over the central Andes, favouring the transport of continental, moist air that is crucial for the development of deep convection over the Altiplano (e.g., Garreaud et al., 2003; Vuille and Keimig, 2004; Falvey and Garreaud, 2005).

Three conspicuous dry regions are observed over the continent (Fig. 2): the Peru–Chile coastal desert, the eastern tip of the continent (Northeast Brazil) and the extratropical plains east of the Andes (southern Argentina, see next section). The first region corresponds to the 100–300 km strip of land between the coastline and the Andes extending from ~30°S as far north as 5°S, and its extreme aridity is due to the large-scale subsidence acting in concert with regional factors (Rutllant et al., 2003). The annual mean precipitation over NE Brazil is only a third of the inland values at the same latitude, restricted to austral fall (when the ITCZ reaches its southernmost position) and highly variable from year-to-year (Rao et al., 1993; Nobre and Shukla, 1996). The aridity of this region seems to result from the local intensification of the Hadley cell in connection with strong convection over the equatorial Atlantic (Moura and Shukla, 1981). Modelling studies also suggest that the heating of Africa is associated with a marked decrease in precipitation over NE Brazil due to low-level moisture divergence and dry-air advection (Cook et al., 2004).

3.2. Extratropical features

South of 40°S, low-level westerly flow prevails year round over the adjacent oceans and the continent (albeit weaker there), in connection with a mean poleward decrease in pressure (Fig. 2a and b). The monthly mean charts, however, don't reflect the high day-to-day variability of the pressure and wind observed in the extratropics; the region is populated by migratory surface cyclones and anticyclones, an integral part of the baroclinic eddies. The midlatitude westerlies extend trough the entire troposphere reaching a maximum speed (the jet stream) in the upper troposphere (Fig. 2c and d). The belt of westerlies is largely symmetric over the Southern Hemisphere, due to the absence of significant land masses to the south of 35°S, and has a rather modest annual cycle (e.g., Nakamura and Shimpo, 2004). In particular, over the southern tip of South America and the adjacent south Pacific, the westerlies are strongest during austral summer, peaking between 45° and 55°S. During the austral winter, the jet stream moves into subtropical latitudes (its axis is at about 30°S) and the low-level westerlies expand equatorward but weaken, particularly at ~50°S (Fig. 3a).

Precipitation over extratropical South America exhibits a marked zonal asymmetry, with very wet (dry) conditions to the west (east) of the Andes cordillera. The rainy western seaboard is connected with a band of precipitation that extends across much of the southern Pacific. In this latter region, most of the rainfall is produced by deep stratiform clouds that develop along warm and cold fronts. The frontal systems are in turn associated with migratory surface cyclones. Although each midlatitude storm exhibits a unique evolution, they tend to drift eastward along rather narrow latitudinal bands known as storm tracks (e.g., Trenberth, 1991; Hoskins and Valdes, 1990; Garreaud, 2007), whose mean position follows the upper-level jet stream. Thus, the area affected by midlatitude precipitation over western South America expands up to about 30°S (central Chile) in winter and then retracts to the south of 40°S during summer (Fig. 3b).

In addition to the frontal precipitation, uplift of low-level winds over the western slope of the Andes produces orographic precipitation leading to a local maximum there (continental precipitation is 2 to 3 times larger than the corresponding oceanic values). In contrast, forced subsidence over the eastern side of the Andes produces very dry conditions in Argentina's Patagonia. Significant frontal rainfall reappears near the Atlantic seaboard and is the major source of winter precipitation as far north as southern Brazil. Over the Atlantic, both the SH transient frontal system and mean low-level convergence lead to the formation of a diagonal band of precipitation maxima, known as the South Atlantic Convergence Zone (SACZ; Kodoma, 1992; Liebmann et al., 1999; Carvalho et al., 2004). In contrast, the zonally oriented Atlantic ITCZ resides farther north and is more affected by wave activity originating in North America (Kiladis and Weickmann, 1997). The SACZ is evident year round but more intense during summer when it is connected with the area of convection over the central part of the continent, producing episodes of intense rainfall over much of southeastern South America (Liebmann et al., 1999). At intraseasonal timescales, the SACZ is part of a see-saw of precipitation over eastern South America (Nogues-Paegle and Mo, 1997; Díaz and Aceituno, 2003). Periods of enhanced SACZ activity are associated with an excess of precipitation in its core and the southern coast of Brazil and drier than normal conditions farther south (northern Argentina, Paraguay and Uruguay). Roughly symmetric but opposite conditions prevail during the weak SACZ periods. At interannual timescales SACZ variability is associated with an anomalous upper-tropospheric, large-scale stationary eddy in the lee of the Andes (Robertson and Mechoso, 2000), which in turn is significantly correlated with SST anomalies over the South Atlantic.

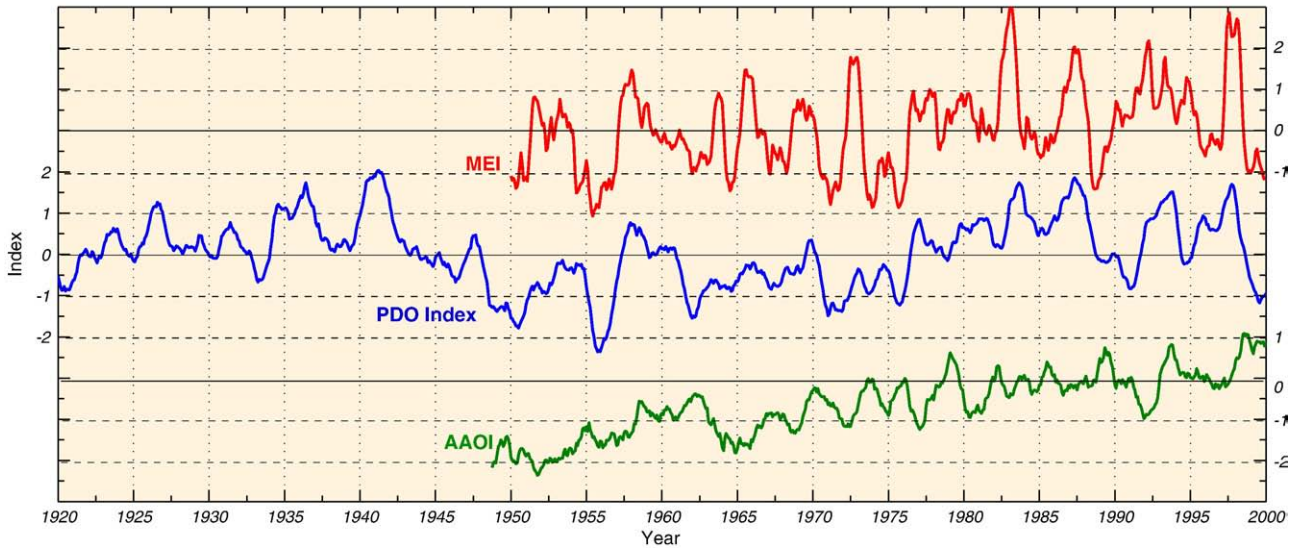

Fig. 5. Time series (1920–2000) of monthly mean Multivariate ENSO Index (MEI), PDO Index and AAO Index. All indexes were smoothed using a 5-month running mean filter. Original indices obtained from Climate Diagnostic Center (NOAA).

Please cite this article as: Garreaud, R.D., et al., Present-day South American climate, Paleogeogr. Palaeoclimatol. Palaeoecol. (2008), doi:10.1016/j.palaeo.2007.10.032

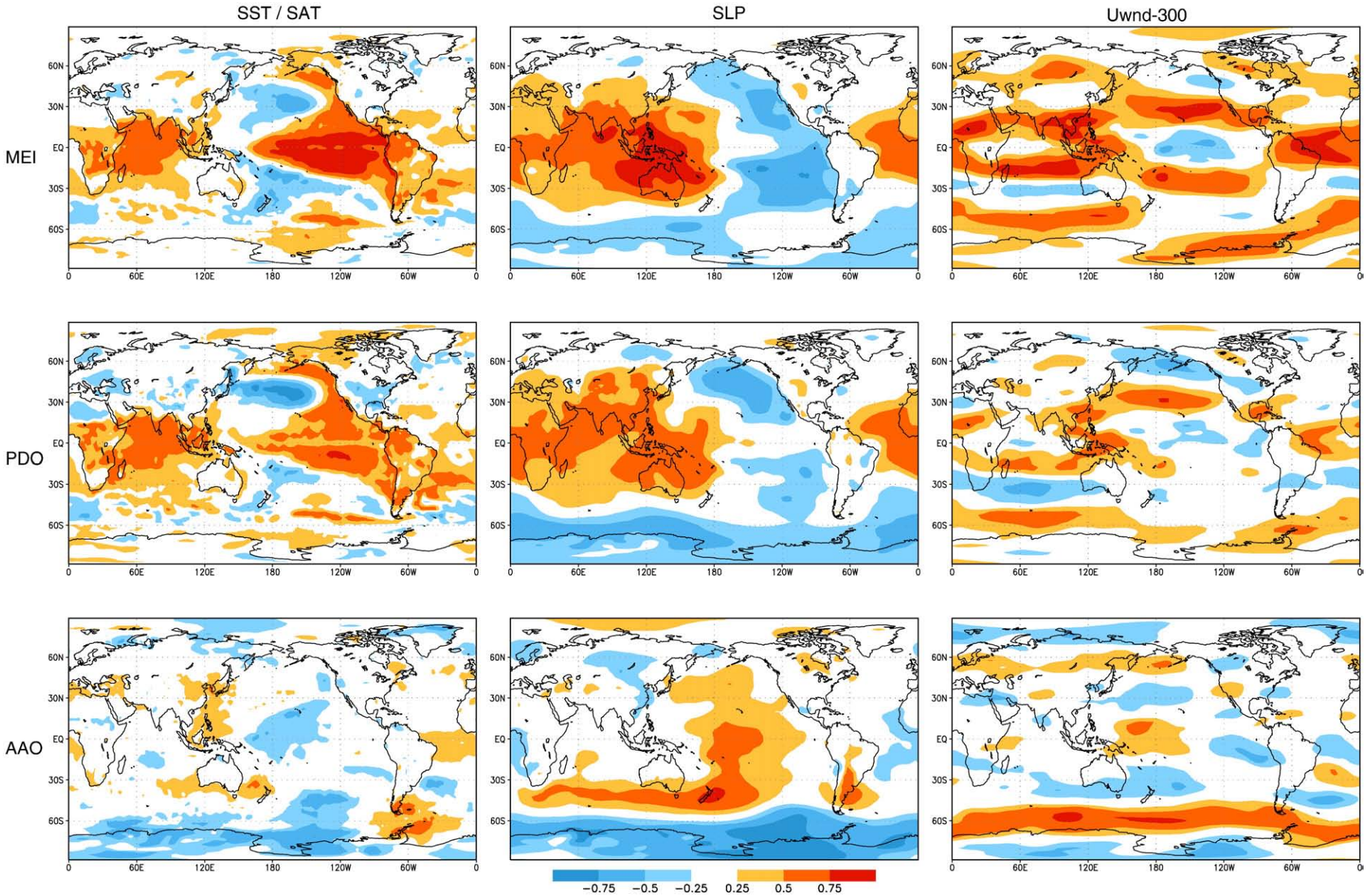

Fig. 6. Spatial fingerprints of the leading atmospheric modes. Upper panels: correlation between the Multivariate ENSO Index (MEI) and Skin Temperature (SST over the ocean, SAT over continents, left panel), sea level pressure (SLP, middle panel) and 300 hPa zonal wind (Uwnd, right panel). Middle panels: as before but for the Pacific Decadal Oscillation (PDO) index. Lower panels: as before but for the Antarctic Oscillation (AAO) index. In all cases, the correlation was calculated using annual mean values for the period 1950–2005.

Please cite this article as: Garreaud, R.D., et al., Present-day South American climate, Paleogeogr. Palaeoclimatol. Palaeoecol. (2008), doi:10.1016/j.palaeo.2007.10.032

3.3. The low-level thermal field

The low-level air temperature field over South America is dominated by the equator-to-pole thermal gradient. Fig. 4a shows the 925-hPa annual mean air temperature averaged between 100° and 20°W ([*T*]). The temperature profile is quite flat (~20 °C) within the tropical belt (20°N–20°S) and then temperature gradually decreases poleward down to 0 °C over the southern tip of the continent. Superimposed on this north–south mean trend, the temperature field also exhibits significant east–west asymmetries, illustrated in Fig. 4b by the zonal anomalies of temperature (at each point, [*T*] was subtracted from the annual mean temperature value). There are negative anomalies over the subtropical Pacific and the adjacent coastal areas and positive anomalies over the interior of the continent. At 20°S, for instance, the Pacific seaboard is about 6° cooler than the Bolivian lowlands just to the east of the Andes and 4 °C cooler than the Atlantic seaboard (this contrast is even more marked when considering summer mean temperatures). The cold air anomaly over the subtropical eastern Pacific is maintained by the upwelling of cold waters along the coast (forced in turn by the low-level southerly winds) and the existence of a persistent, extensive deck of low-level stratocumulus clouds reflecting more than 60% of the incoming solar radiation (e.g., Klein and Hartmann, 1993).

The mean annual cycle of the low-level air temperature also exhibits interesting regional features, partially illustrated in Fig. 4c by the January–July mean temperature difference. This difference maximizes near 40°S to the east of the Andes (over +12 °C), rapidly decreasing equatorward and reversing its sign over the southern Amazon Basin (where July is warmer than January). This latter behaviour is explained by the summertime development of clouds (shading the surface from sunlight) and rainfall (moistening the surface) over the central part of the continent, where maximum temperatures tend to occur just before the onset of the rainy season.

4. Interannual variability

Superimposed on the mean annual cycle the atmospheric conditions exhibit non-regular fluctuations on a wide range of temporal scales. On sub-monthly timescales, the fluctuations tends to exhibit a quasi-weekly periodicity associated with the passage of midlatitude disturbances that owe their existence to the baroclinic instability of the tropospheric flow. Atmospheric fluctuations on longer timescales include intraseasonal (20–60 days), interannual and interdecadal variability. They arise from the relatively slow changes imposed by the boundary conditions, passed on to the atmosphere through anomalous surface fluxes of heat, moisture and momentum. Regional or local-scale changes are extended over the globe by the atmospheric circulation and eventually feed back into the original source. Different analysis techniques and datasets have yielded a large number of patterns of atmospheric variability (termed teleconnections, oscillation, dipoles, etc.), but it seems that most of the low-frequency variance resides in a few global modes (e.g., Quadrelli and Wallace, 2004): ENSO, the Pacific Decadal Oscillation (PDO, Mantua et al., 1997), and the Arctic and Antarctic Annular Modes (AO and AAO, Thompson and Wallace, 2000), besides the Madden–Julian Oscillation (MJO, see Madden and Julian 1994 for a review) which is responsible for most of the intraseasonal variability over much of the tropics and subtropics. Its impacts on South America are reviewed in Nogués-Paegle et al. (2000). The temporal evolution of these modes is presented in Fig. 5 by the time series of representative indices. The spatial fingerprints of these modes are presented in Fig. 6 by global maps of correlation between the indices and the SST, SLP and upper-level winds.

Before we address the impact of each global mode, it is worthwhile to gauge the amplitude of the interannual variability of temperature and precipitation over South America. Fig. 4d shows the standard deviation of the annual mean temperature at 925 hPa (that is one value per year, 50 yr in total). Over the tropics (including the Amazon basin) the year-to-year variations are modest (~0.8 °C) but they are about half the amplitude of the mean annual cycle (compare Fig. 4c and d). Over the subtropical plains the year-to-year variations are large (~1.6 °C) but they are only a fifth of the mean annual cycle. The standard deviation of the annual precipitation (Fig. 7a) ranges from 50 to 500 mm. The maximum values are found over the Amazon basin (particularly over the Atlantic seaboard) and southern Chile; the minimum are found over Argentina's Patagonia. In the case of precipitation, it is useful to normalize the interannual standard deviation by the annual mean (Fig. 7b). When doing so, it results that year-to-year fluctuations over the Amazonia and southern Chile are a

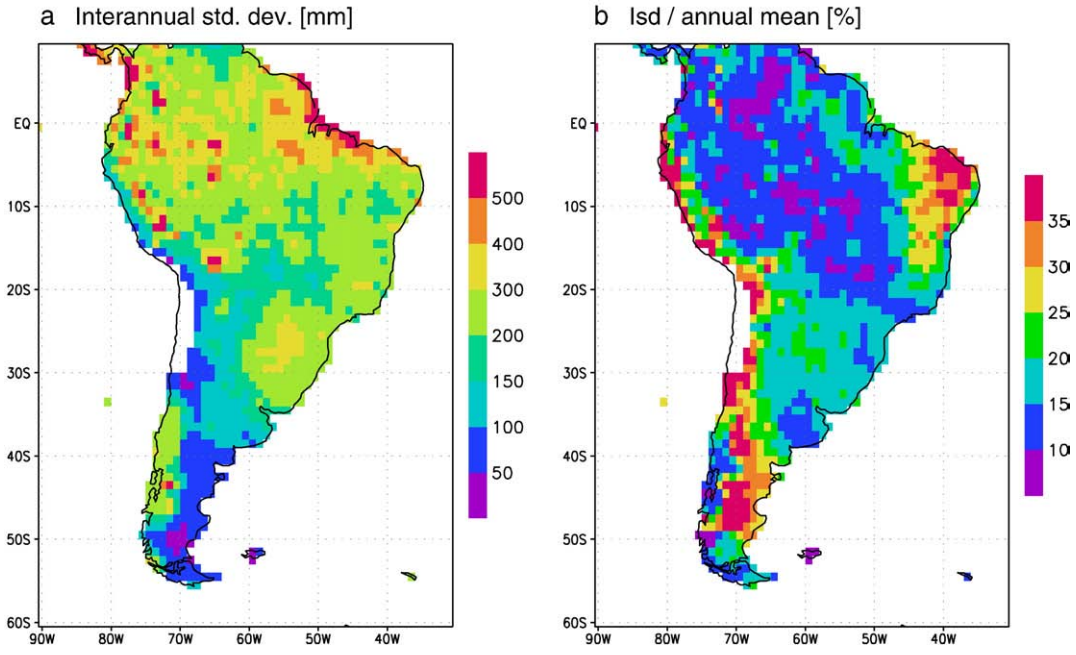

Fig. 7. (a) Standard deviation of the annual mean precipitation (University of Delaware gridded dataset). (b) Standard deviation of the annual mean precipitation normalized by the annual mean precipitation. Standard deviation and ratio are not shown where the annual mean value is less than 50 mm.

Please cite this article as: Garreaud, R.D., et al., Present-day South American climate, Paleogeogr. Palaeoclimatol. Palaeoecol. (2008), doi:10.1016/j.palaeo.2007.10.032

Table 2
ENSO-related anomalies in precipitation in different regions of South America

Region	Key references	Sign season	Basic mechanism
Northern South America (Colombia, Venezuela)	Poveda et al. (2001) Acevedo et al. (2001)	– – DJF	Decrease in convection due to relaxed land–sea thermal contrast and extra subsidence from convection over the ITCZ
Coastal northern Peru/ southern Ecuador	Horel and Cornejo-Garrido (1986) Goldberg et al. (1987)	++ JFMAM	Development of deep convection due to anomalously warm SST
Tropical Andes	Francou et al. (2004) Vuille et al., (2000a)	– DJFMA	Subdued convection due to shift and weakening of Walker circulation
Altiplano (central Andes)	Vuille 1999 Vuille et al. (2000b) Garreaud and Aceituno (2001)	– DJF	Decrease in advection of moist air from the continent due to stronger mid-level westerly flow
Bolivian lowlands	Ronchail and Gallaire (2006)	– DJFM	Basic mechanism unknown (changes in the low-level jet?)
Subtropical Andes and central Chile	Rutllant and Fuenzalida (1991) Montecinos and Aceituno (2000) Masiokas et al. (2006)	++ JJAS	Increase in midlatitude storms over subtropical latitudes due to blocking in the southeast Pacific
Southern Chile	Montecinos and Aceituno (2000)	– NDJ	Decrease in midlatitude storms due to nearby blocking in the southeast Pacific
Argentina's Patagonia	Compagnucci and Araneo (2007)	+ JJASON	Indirect effect due to changes in SST at higher latitudes and concomitant changes in evaporation and atmospheric moisture
Southeastern South America (SESA)	Grimm (2003) Silvestri (2005) Barros and Silvestri (2002)	++ SON	Increase in baroclinic activity due to enhanced subtropical jet stream
Amazon basin	Marengo (1992) Liebmann and Marengo (2001) Ronchail et al. (2002)	– DJF	Intense convection over the tropical Pacific leads to enhanced subsidence and rainfall suppression over central Amazonia
NE Brazil	Folland et al. (2001) Giannini et al. (2001) Nobre and Shukla (1996)	– MAM	ENSO projects upon a warm (cold) tropical north (south) Atlantic pattern, leading to reduction of convection over NE Brazil

Notes:
Sign refers to the correlation between ENSO index and regional precipitation. + (−) indicates wetter (drier) conditions during El Niño (La Niña) events. Double (single) sign is for strong (weak) relationship.
Season indicates the period of the year in which the previous relationship is strongest.

small fraction (less than 15%) of the corresponding annual mean. In contrast, year-to-year variations can be as large as one third of the annual mean over NE Brazil, central Chile, the northern coast of Peru and southern Argentina. Scientists must be aware of such discrepancies between absolute and relative measurements of interannual variability when considering the impact of climate fluctuations on other systems.

4.1. ENSO-related variability

ENSO is a coupled ocean-atmosphere phenomenon rooted in the tropical Pacific, characterized by irregular fluctuations between its warm (El Niño) and cold (La Niña) phases with a periodicity ranging from 2 to 7 yr (see Diaz and Markgraf, 1992 for a review on ENSO). Rainfall and temperature anomalies associated with occurrence of the El Niño and La Niña events are the major source of interannual variability over much of South America (e.g., Ropelewski and Halpert, 1987; Aceituno, 1988; Kiladis and Diaz, 1989; Marengo, 1992). Not surprisingly, ENSO-related variability has received considerable attention, and Table 2 shows an incomplete list of studies documenting and diagnosing the effect of ENSO on specific regions.

In order to summarize these effects, Fig. 8 shows seasonal maps of the correlation between the Multivariate ENSO Index (MEI; Wolter and Timlin, 1998) and the gridded precipitation and surface air temperature fields. The overall pattern is that El Niño episodes (positive MEI) are associated with: (a) below normal rainfall over tropical South America, (b) above normal precipitation over the southeastern portion of the continent and central Chile, and (c) warmer than normal conditions over tropical and subtropical latitudes. Opposite rainfall and temperature anomalies are observed during La Niña episodes. Partly because of the limited spatial resolution of the precipitation datasets, some details of the ENSO forcing are not well represented in Fig. 8, especially over areas of complex terrain. For instance, flooding conditions along the semi-arid coast of southern Ecuador and northern Peru at the peak of El Niño episodes are very evident in the few station records there but barely distinguishable in Fig. 8. Similarly, use of high-resolution cold cloudiness data indicates that precipitation variability in the central Andes shows less spatial coherence than apparent from Fig. 8, with many years showing an alternation of wet/dry conditions between the northern and southern part of the study area (Vuille and Keimig, 2004).

Closer inspection of Fig. 8 reveals significant seasonal changes in the precipitation-MEI regression field. The maximum correlation (either positive or negative) is reached at the height of the corresponding rainy season over the semi-arid regions of NE Brazil (MAM), the Altiplano (DJF) and central Chile (JJA), as well as over the more humid southeastern South America (SON). In contrast, the largest (negative) correlations over the equatorial Andes and the Guiana Highlands are found during DJF, which coincides with one minimum of the semi-annual cycle in those regions. Over the Amazon Basin negative correlations are strong (weak) in the eastern (western) side and tend to maximize during JJA. Further details on the seasonality of ENSO-related rainfall and streamflow anomalies are presented by Montecinos et al. (2000), Grimm et al. (2000), Cazes-Boezio et al. (2003), Compagnucci and Vargas (1998) and Compagnucci (2000) for subtropical South America, and by Liebmann and Marengo (2001) and Marengo and Nobre (2001) for the Amazon basin. Seasonal changes are also evident in the MEI-temperature correlation maps. The positive correlations over tropical South America maximize around December–March (particularly on its western side), because ENSO-related SST anomalies over the adjacent tropical Pacific reach their maximum amplitude in those months (ENSO phase locking). Cold air anomalies during El Niño events are observed over midlatitudes during spring, likely because an ENSO-related increase

Fig. 8. Seasonal correlation map between MEI and precipitation (upper row) and surface air temperature (lower row). Gridded fields from University of Delaware (1950–1999). Only correlations in excess of ±0.2 are shown (roughly the threshold of the 95% significance level).

Please cite this article as: Garreaud, R.D., et al., Present-day South American climate, Paleogeogr. Palaeoclimatol. Palaeoecol. (2008), doi:10.1016/j.palaeo.2007.10.032

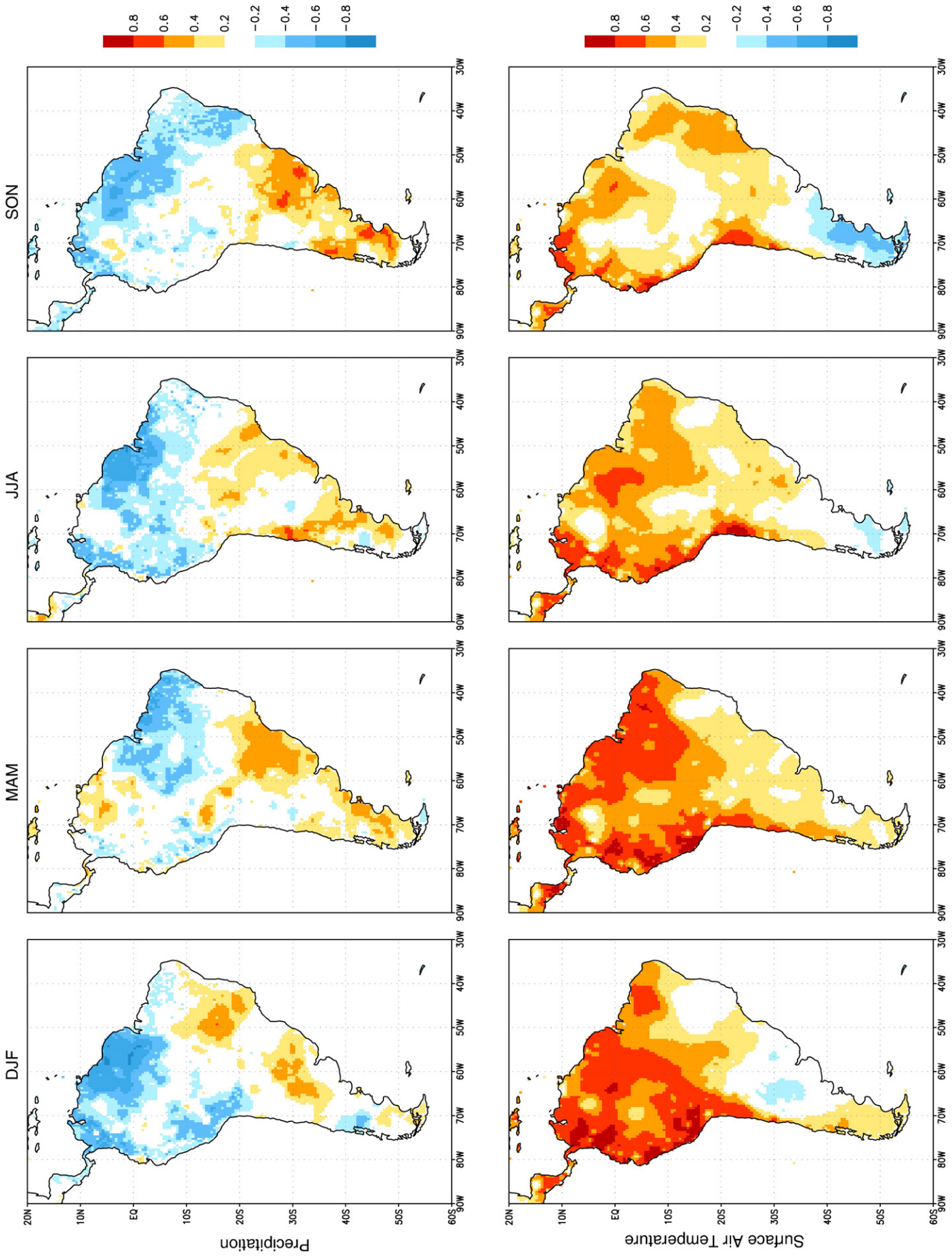

Please cite this article as: Garreaud, R.D., et al., Present-day South American climate, Paleogeogr. Palaeoclimatol. Palaeoecol. (2008), doi:10.1016/j.palaeo.2007.10.032

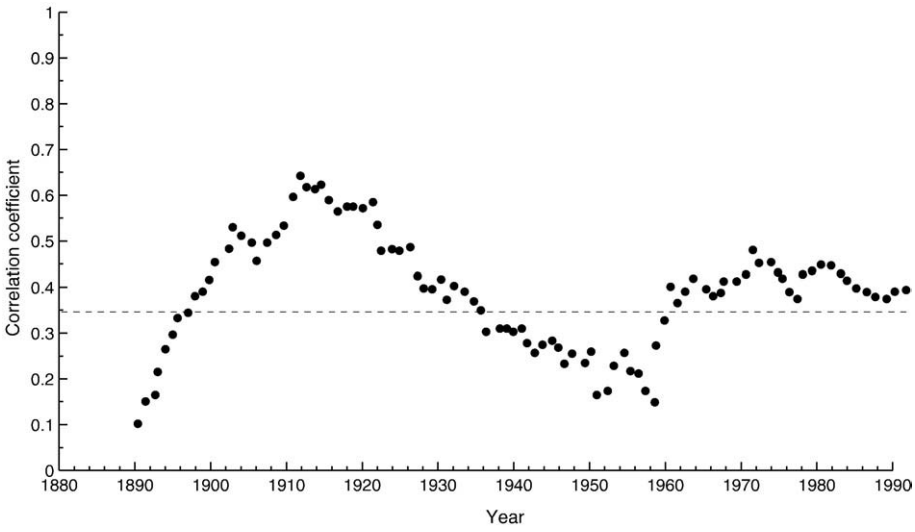

Fig. 9. Time series of the correlation coefficient between October–November–December precipitation at Corrientes (27.5°S 65.6°W) and the contemporaneous Southern Oscillation Index (SOI) considering a 30-year sliding window. The values are assigned to the 15th year within the corresponding 30-year window. The horizontal dashed line indicates the 95% significance level. Adapted and updated from Aceituno and Montecinos (1993).

in rainfall is also associated with a reduction of insolation and moistening of the surface.

The previously described correlation analysis gives us information on the relationship between ENSO and local interannual variability based on the complete record for the last 50 yr. Note that the largest values in the correlation maps are about ~0.8, so that ENSO explains two thirds of the interannual variance of precipitation/temperature at the most. Part of the scatter stems from the variations in precipitation anomalies among different warm (or cold) events that cannot be purely associated with the variability of tropical SST (e.g., Marengo et al., 2008; Vera et al., 2004). Furthermore, the amplitude of the ENSO-related anomalies can experience significant changes on decadal and longer timescales, because either other factors are at play (eclipsing ENSO-related anomalies), changes in ENSO behaviour (e.g., a shift in its seasonal phase-lock), or changes in the basic-state, which alter ENSO-related teleconnections over the extratropics. Indeed, changes in ENSO behaviour have been noted in the last century (e.g., Elliott and Angell, 1988). Aceituno and Montecinos (1993) calculated the correlation coefficient between the sea level pressure at Darwin (an index of the Southern Oscillation) and precipitation at 7 stations over South America, using a 30-year sliding window from 1880 to 1990. While the sign of the correlation didn't change during the century, its statistical significance varied from null to high. For instance, spring precipitation at Corrientes (27°S 65°W) is positively correlated with the Southern Oscillation, but the association is statistically significant (at the 95% confidence level) only from 1900–1920 and from 1960 onwards (Fig. 9). This non-stationarity adds uncertainty when extrapolating the present-day relationship between ENSO and interannual climate variability into the past.

4.2. PDO-related variability

Precipitation records over South America also exhibit decadal and interdecadal variability, although its amplitude is smaller than (typically less than 10% of) the year-to-year changes. Keep in mind that only a few stations have century-long records on South America, limiting our ability to detect interdecadal changes and characterize their spatial patterns. Interdecadal variability in NE Brazil has been associated with SST anomalies in the tropical Atlantic as well as low-frequency changes in the North Atlantic Oscillation (e.g., Nogués-Paegle and Mo, 2002). Otherwise, the most plausible forcing behind these low-frequency fluctuations is the Pacific Decadal Oscillation (PDO), a long-lived pattern of Pacific climate variability (e.g., Mantua et al., 1997). The PDO is often described as ENSO-like, because the spatial climate fingerprints of its warm and cold phase have strong resemblance with those of El Niño and La Niña events, respectively (e.g., Garreaud and Battisti, 1999; see also Fig. 6). The causes of the PDO and its links with ENSO are not fully understood yet (Newman et al., 2003; Schneider and Cornuelle, 2005).

In order to compare the PDO-related and ENSO-related anomalies, Fig. 10 shows the annual mean precipitation and temperature fields regressed upon MEI and PDO index. The PDO index is defined as the leading principal component of the North Pacific (north of 20°N) monthly SST variability. The value of the regression coefficient R (whereby R is defined at each grid box as R(lat,long)=r(lat,long) σ_F (lat,long)/σ_I, where r(lat,long) is the local correlation coefficient between the index and the field, σ_F(lat,long) is the standard deviation of the field and σ_I is the standard deviation of the index), indicates the local anomalies in the field (in physical units: mm or °C) associated with a unit anomaly of the index. It turns out that PDO-related anomalies of precipitation and temperature over South America are also ENSO-like (i.e., similar spatial structure), but their amplitude is about half of their ENSO counterparts.

Several studies have documented a significant increase in precipitation and riverflow over southeastern South America, southern Amazonia, (e.g., Genta et al., 1998; García and Vargas, 1998; Robertson and Mechoso, 2000) and for the eastern Andean rivers (Wylen et al., 2000; Compagnucci et al., 2000) together with a decrease in rainfall over northern Amazonia (e.g., Marengo, 2004) after 1976/77, relative to the previous two decades. This "climate shift" is consistent with the change in polarity of the PDO (from cold to warm) in the mid 70s (Fig. 5), but can't be exclusively attributed to the PDO variability because El Niño events have also become more frequent and intense in the 80s and 90s compared with the previous three decades. In an alternative approach, Andreoli and Kayano (2005) considered the PDO as a low-frequency modulator of the ENSO-related variability and found a "constructive interference": El Niño (La Niña) rainfall anomalies tend to be stronger in those episodes that occurred during the warm (cold) phase of the PDO.

4.3. AAO-related anomalies

The Antarctic Oscillation (AAO), also known as the Southern Hemisphere Annular Mode, is the leading pattern of tropospheric circulation variability south of 20°S, and it is characterized by pressure anomalies of one sign centered in the Antarctic and anomalies of the

Please cite this article as: Garreaud, R.D., et al., Present-day South American climate, Paleogeogr. Palaeoclimatol. Palaeoecol. (2008), doi:10.1016/j.palaeo.2007.10.032

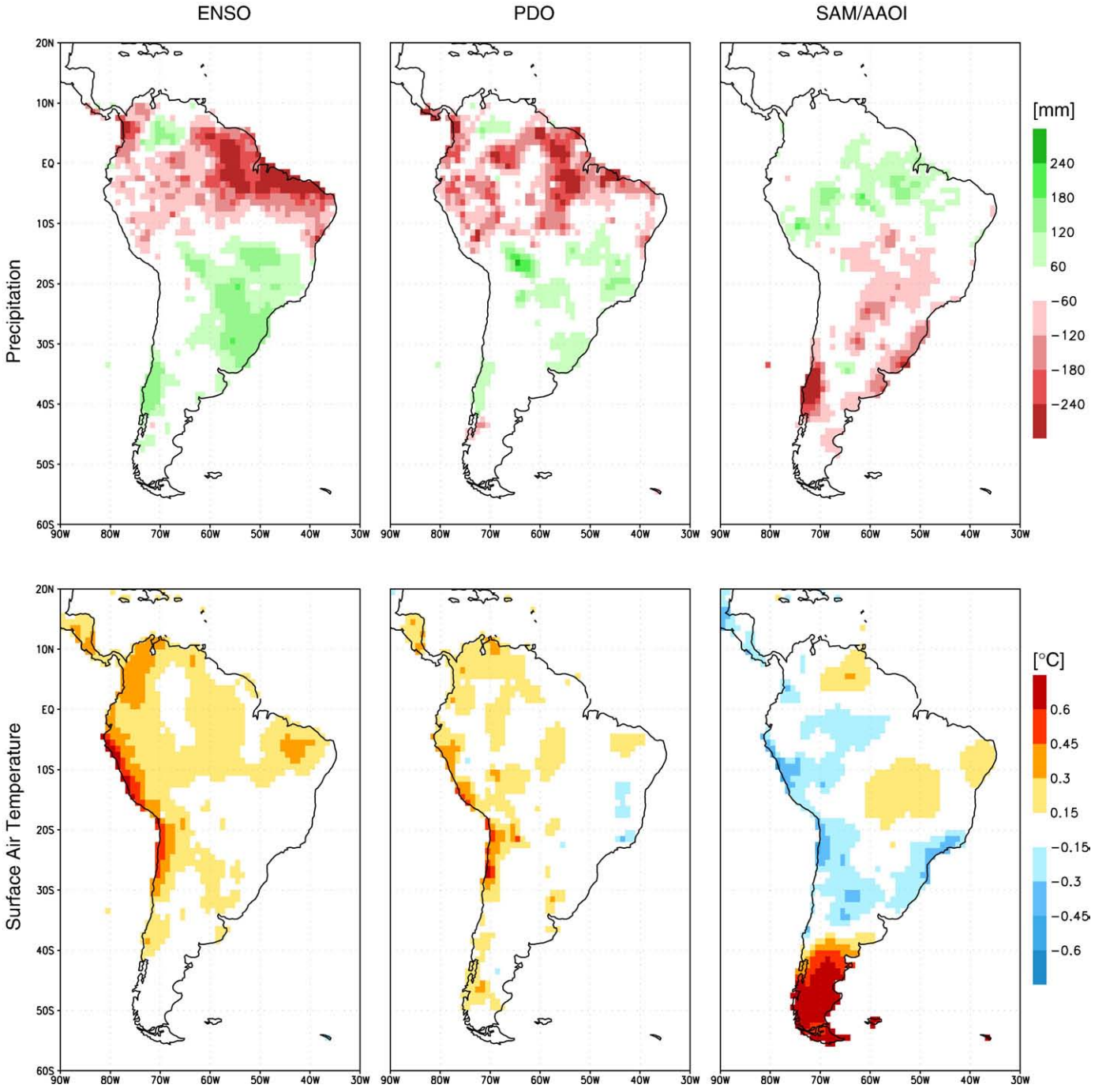

Fig. 10. Annual mean precipitation (upper row) and surface air temperature (lower row) regressed upon MEI (left column), PDO index (center column) and AAOI (right column). Precipitation and surface air temperature from University of Delaware gridded dataset.

opposite sign on a circumglobal band at about 40–50°S (Kidson, 1988; Thompson and Wallace, 2000, see also Fig. 6). The AAO is largely zonally symmetric, its signal extends coherently up to the lower-stratosphere, and it seems to arise from the interaction between the eddies and the zonal mean flow (e.g., Codron, 2005). The positive phase of the AAO is associated with decreased (increased) surface pressure and geopotential heights over Antarctica (midlatitudes) and a strengthening and poleward shift of the SH westerlies. Opposite conditions prevail during the negative phase. There are several indices to characterize the AAO; here we use the leading principal component of the 850 hPa geopotential height anomalies to the south of 20°S (Fig. 5). The AAO Index has considerable variance at intermonthly and interannual timescales, superimposed on a marked trend toward its positive phase in the last 50 yr. Such a trend is consistent with a reduction in the stratospheric ozone levels at high-latitudes (Thompson and Solomon, 2002). At sub-monthly timescales, the negative (positive) phase of the AAO are dominant when SST and convection anomalies resemble El Niño (La Niña) phases of ENSO and/or there is enhanced tropical intraseasonal variability (Carvalho et al., 2005).

The annual mean precipitation and temperature were also regressed upon the AAOI (Fig. 10). In this case, the AAOI was previously detrended, so the regression only accounts for the covariability at interannual timescales (and not from a common trend). There is a large response of the surface air temperature to the south of 40°S, such that warming is associated with the positive phase of the AAO. The large-scale warming is largest in austral summer (not shown), also evident

Please cite this article as: Garreaud, R.D., et al., Present-day South American climate, Paleogeogr. Palaeoclimatol. Palaeoecol. (2008), doi:10.1016/j.palaeo.2007.10.032

elsewhere between 40° and 60°S (e.g., Gillett et al., 2006) and produced by a combination of enhanced horizontal advection, subsidence and solar radiation (Gupta and England, 2006). AAO-related precipitation anomalies are significant in southern Chile (largest at 40°S) and along the subtropical east coast of the continent (see also Gillett et al., 2006). In the former place, the decrease in precipitation during the positive phase of the AAO can be explained in terms of a reduction of the zonal flow at midlatitudes, which translates in less frontal and orographic precipitation in that region Garreaud, 2007). The negative correlation between AAOI and SESA rainfall is largest during spring and associated with a weakening of the moisture convergence (Silvestri and Vera, 2003). In this area, AAO activity produces a strong modulation of the ENSO signal on precipitation.

5. Concluding remarks

- Consistent with its extension from 10°N down to about 53°S, South America exhibits tropical, subtropical and extratropical climatic features. Superimposed on the mean north-to-south variations, there are significant east–west asymmetries across the continent forced by the presence of the Andes, changes in the continental width (broad at low latitudes narrow at midlatitudes) and the boundary conditions imposed by a cold southeastern Pacific and a warm south-western Atlantic. Thus, at tropical and subtropical latitudes, dry and relatively cold conditions prevail along the Pacific seaboard and the narrow strip of land to the east of the Andes. In contrast, warm and humid conditions prevail over the interior of the continent all the way from the Andes foothills westward to the Atlantic seaboard. The rainy conditions over the central part of the continent maximize during summer (the South American Monsoon season) and support the world's largest rainforest over the Amazon basin. In this season, part of the water vapour recycled over Amazonia is transported southward by a low-level jet to the east of the Andes feeding deep convection as far south as 35°S (e.g., La Plata basin). Notice that continental Monsoon, the oceanic ITCZ, and the SACZ are different (albeit related) systems.
- At extratropical latitudes precipitation is mostly caused by mid-latitudes storms moving westward along the storm tracks at about 40–50°S. The mean latitudinal position of the storm tracks follows closely the axis of the westerly wind maxima in the middle and upper troposphere. Again, the presence of the Andes significantly disrupts the precipitation pattern with very wet (dry) conditions to the west (east) of the range. West of the Andes, uplift of moist air leads to significant orographic rainfall that act in concert with frontal precipitation. In contrast, forced subsidence over the eastern side of the Andes produces dry conditions in Argentina's Patagonia; significant frontal rainfall only reappears near the Atlantic seaboard.
- Among the many factors that determine the interannual climate variability in South America, ENSO plays a major role in many regions. Studies of ENSO-related rainfall anomalies at a global scale indicate that the El Niño episodes are typically associated with below normal rainfall and warmer than normal conditions in the northern part of South America, as well as anomalously wet conditions in the southeastern portion of the continent and central Chile. Opposite rainfall anomalies are typically observed in both regions during La Niña events. This large picture of the ENSO impacts on rainfall in South America exhibits considerable variation when analyzed at a regional scale and significant seasonal fluctuations. Furthermore, the strength of the relation between ENSO and regional climate has shown considerable variability during the 20th century, possible because of changes in ENSO behaviour and/or the influence of other factors.
- Decadal and interdecadal variability is also evident in many records across the continent, and possibly forced by the Pacific Decadal Oscillation (PDO). PDO-related anomalies of precipitation and temperature over South America have a spatial structure similar to those related to ENSO, but with smaller amplitude. In particular, a prominent "climate shift" around the mid 70s, evident in many hydro-meteorological variables, is consistent with the change in polarity of the PDO (from cold to warm). The differences in mean climate before and after the shift can't be exclusively attributed to the PDO variability because El Niño events have also became more frequent and intense in the 80s and 90s compared with the previous three decades.
- Another source of low-frequency variability is the Antarctic Oscillation (AAO), characterized by pressure anomalies of one sign centered in the Antarctic and anomalies of the opposite sign on a circumglobal band at about 40–50°S. There is a large response of the surface air temperature to the south of 40°S, such that warming is associated with the positive phase of the AAO. AAO-related precipitation anomalies are significant in southern Chile (largest at 40°S) and along the subtropical east coast of the continent.

Acknowledgments

The authors thank R. Villalba and M. Grosjean for the organization of the PAGES meeting in Malargue that inspired this work. RG was supported by CONICYT (Chile) grant ACT-19. MV was supported by NSF EAR-0519415. RC is funded by Proyecto de Investigación Plurianual CONICET (PIP 5006), Proyectos AGENCIA PICT2004-26094 y PICTR2002-00186 y Proyecto UBACYT X095. JM is funded by MMA/BIRD/GEF/CNPq (PROBIO Project), the UK Global Opportunity Fund-GOF Project Using Regional Climate Change Scenarios for Studies on Vulnerability and Adaptation in Brazil and South America, and the CLARIS-EU project.

References

Aceituno, P., 1988. On the functioning of the Southern Oscillation in the South American sector. Part I: surface climate. Mon. Weather Rev. 116, 505–524.
Aceituno, P., Montecinos, A., 1993. Stability analysis of the relationship between the Southern Oscillation and rainfall in South America. Bull. Inst. Fr. Etudes Andines 22, 53–64.
Acevedo, M., McGregor, K., Andressen, R., Ramirez, H., 2001. Relations of climate variability in Venezuela to tropical Pacific SST anomalies. Final Proc. 10th Symposium on Global Change Studies, American Meteorological Society. San Antonio Texas, USA, pp. 1.31–1.36.
Adler, R., Huffman, G.J., Chang, A., Ferraro, R., Xie, P.P., Janowiak, J., Rudolf, B., Schneider, U., Curtis, S., Bolvin, D., Gruber, A., Susskind, J., Arkin, P., Nelkin, E., 2003. The Version-2 Global Precipitation Climatology Project (GPCP) Monthly Precipitation Analysis (1979–Present). J. Hydrometeorol. 4, 1147–1167.
Andreoli, R., Kayano, M., 2005. ENSO-related rainfall anomalies in South America and associated circulation features during warm and cold Pacific Decadal Oscillation regimes. Int. J. Climatol. 25, 2017–2030.
Barros, V., Silvestri, G.E., 2002. The relation between sea surface temperature at the subtropical south-central Pacific and precipitation in southeastern South America. J. Climate 15, 251–267.
Barros, V., Castañeda, M.E., Doyle, M., 2000. Recent precipitation trends in southern South America east of the Andes: an indication of climatic variability. In: Smolka, P.P., Volkheimer, W. (Eds.), Southern Hemisphere Paleo and Neo-Climates: Methods and Concepts. Springer, Berlin, pp. 325–375.
Carvalho, L., Jones, C., Liebmann, B., 2004. The South Atlantic Convergence Zone: intensity, form, persistence, and relationships with intraseasonal to interannual activity and extreme rainfall. J. Climate 17, 88–108.
Carvalho, L., Jones, C., Ambrizzi, T., 2005. Opposite phases of the Antarctic Oscillation and relationships with intraseasonal to interannual activity in the tropics during the austral summer. J. Climate 18, 702–718.
Cazes-Boezio, G., Robertson, A.W., Mechoso, C.R., 2003. Seasonal dependence of ENSO teleconnections over South America and relationships with precipitation in Uruguay. J. Climate 16, 1159–1176.
Chen, T.C., Weng, S.P., Schubert, S., 1999. Maintenance of austral summertime upper-tropospheric circulation over tropical South America: The Bolivian High–Nordeste Low System. J. Atmos. Sci. 56, 2081–2100.
Codron, F., 2005. Relation between annular modes and the mean state: southern hemisphere summer. J. Climate 18, 320–330.
Compagnucci, R.H., 2000. ENSO events impact on hydrological system in the Cordillera de los Andes during the last 450 years. In: Smolka, P.P., Volkheimer, W. (Eds.), Southern Hemisphere Paleo and Neo-Climates: Methods and Concepts. Springer, Berlin, pp. 175–185.
Compagnucci, R.H., Araneo, D., 2007. Alcances de El Niño como predictor de el caudal de los ríos andinos argentinos. Ing. Hidraul. Mex. 22 (3), 23–35.
Compagnucci, R.H., Vargas, W., 1998. Interannual variability of Cuyo Rivers streamflow in Argentinean Andean Mountains and ENSO events. Int. J. Climatol. 18, 1593–1609.
Compagnucci, R.H., Blanco, S.A., Figliola, M.A., Jacovkis, P.M., 2000. Variability in subtropical Andean Argentinean Atuel river: a wavelet approach. Environmetric 11, 251–269.

Please cite this article as: Garreaud, R.D., et al., Present-day South American climate, Paleogeogr. Palaeoclimatol. Palaeoecol. (2008), doi:10.1016/j.palaeo.2007.10.032

Cook, K., Sieh, J.S., Hagos, S.M., 2004. The Africa–South America Intercontinental Teleconnection. J. Climate 17, 2851–2865.

Diaz, H.F., Markgraf, V., 1992. El Niño. Cambridge University Press, Cambridge.

Díaz, A., Aceituno, P., 2003. Atmospheric circulation anomalies during episodes of enhanced and reduced convective cloudiness over Uruguay. J. Climate 16, 3171–3185.

Dima, I., Wallace, J.M., 2003. On the seasonality of the Hadley Cell. J. Atmos. Sci. 60, 1522–1527.

Elliott, W., Angell, J., 1988. Evidence for changes in Southern Oscillation relationships during the last 100 years. J. Climate 1, 729–737.

Falvey, M., Garreaud, R., 2005. Moisture variability over the South American Altiplano during the SALLJEX observing season. J. Geophys. Res. 110, D22105. doi:10.1029/2005JD006152.

Folland, C., Colman, A., Rowell, D.P., Davey, M., 2001. Predictability of Northeast Brazil rainfall and real-time forecast skill, 1987–98. J. Climate 14, 1937–1958.

Francou, B., Vuille, M., Favier, V., Cáceres, B., 2004. New evidence for an ENSO impact on low latitude glaciers: Antizana 15, Andes of Ecuador, 0°28S. J. Geophys. Res. 109, D18106. doi:10.1029/2003JD004484.

Fu, R., Zhu, B., Dickinson, R.E., 1998. How do atmosphere and land surface influence seasonal changes of convection in the tropical Amazon? J. Climate 12, 1306–1321.

García, N., Vargas, W., 1998. The temporal climatic variability in the Río De La Plata Basin displayed by the river discharges. Clim. Change 38, 359–379.

Garreaud, R., 2007. Precipitation and circulation covariability in the extratopics. J. Climate 20, 4789–4797.

Garreaud, R.D., Battisti, D.S., 1999. Interannual (ENSO) and interdecadal (ENSO-like) variability in the Southern Hemisphere tropospheric circulation. J. Climate 2, 2113–2123.

Garreaud, R.D., Aceituno, P., 2001. Interannual rainfall variability over the South American Altiplano. J. Climate 14, 2779–2789.

Garreaud, R.D., Aceituno, P., 2007. Atmospheric circulation over South America: mean features and variability. In: Veblen, T., Young, K., Orme, A. (Eds.), The Physical Geography of South America. Oxford University Press, Oxford, pp. 45–66.

Garreaud, R., Vuille, M., Clement, A., 2003. The climate of the Altiplano: observed current conditions and mechanism of past changes. Paleogeogr. Palaeoclimatol. Palaeoecol. 194 (3054), 1–18.

Genta, J.L., Perez-Iribarren, G., Mechoso, C.R., 1998. A recent increasing trend in the streamflow of rivers in southeastern South America. J. Climate 11, 2858–2862.

Giannini, A., Chiang, J., Cane, M., Kushnir, Y., Seager, R., 2001. The ENSO teleconnection to the tropical Atlantic Ocean: contributions of the remote and local SSTs to rainfall variability in the tropical Americas. J. Climate 14, 4530–4544.

Gillett, N.P., Kell, T.D., Jones, P.D., 2006. Regional climate impacts of the southern annular mode. Geophys. Res. Lett. 33, L23704. doi:10.1029/2006GL027721.

Goldberg, R.A., Tisnado, G., Scofield, R.A., 1987. Characteristics of extreme rainfall events in Northwestern Peru during the 1982–1983 El Nino period. J. Geophys. Res. 92 (C13), 14, 225–14,241.

Grimm, A.M., 2003. The El Niño impact on the summer monsoon in Brazil: regional processes versus remote influences. J. Climate 16, 263–280.

Grimm, A.M., Barros, V., Doyle, M.E., 2000. Climate variability in southern South America associated with El Niño and La Niña Events. J. Climate 13, 35–58.

Gupta, A.S., England, S., 2006. Coupled ocean–atmosphere–ice response to variations in the southern annular mode. J. Climate 19, 4457–4486.

Horel, J., Cornejo-Garrido, A., 1986. Convection along the coast of Northern Peru during 1983. spatial and temporal variation of clouds and rainfall. Mon. Weather Rev. 114, 2091–2105.

Horel, J., Hahmann, A., Geisler, J., 1989. An investigation of the annual cycle of the convective activity over the tropical Americas. J. Climate 2, 1388–1403.

Hoskins, B.J., Valdes, P.J., 1990. On the existence of storm-tracks. J. Atmos. Sci. 47, 1854–1864.

Kalnay, E., Kanamitsu, M., Kistler, R., Collins, W., Deaven, D., Gandin, L., Iredell, M., Saha, D., White, G., Woollen, J., Zhu, Y., Chelliah, M., Ebisuzaki, W., Higgins, W., Janowiak, J., Mo, K.C., Ropelewski, C., Wang, J., Leetma, A., Reynolds, R., Dennis, J., 1996. The NCEP/NCAR 40-years reanalysis project. Bull. Am. Meteorol. Soc. 77, 437–472.

Kidson, J., 1988. Indices of the Southern Hemisphere Zonal Wind. J. Climate 1, 183–194.

Kiladis, G.N., Diaz, H., 1989. Global climatic anomalies associated with extremes in the Southern Oscillation. J. Climate 2, 1069–1090.

Kiladis, G.N., Weickmann, K.M., 1997. Horizontal structure and seasonality of large-scale circulations associated with submonthly tropical convection. Mon. Wea. Rev. 125, 1997–2013.

Kistler, R., et al., 2001. The NCEPNCAR 50 year reanalysis. Bull. Am. Meteorol. Soc. 82, 247–267.

Klein, S.A., Hartmann, D.L., 1993. The seasonal cycle of low stratiform clouds. J. Climate 6, 1587–1606.

Kodoma, Y., 1992. Large-scale common features of subtropical precipitation zones (the Baiu frontal zone, the SPCZ and the SACZ). Part I: characteristic of subtropical frontal zones. J. Meteorol. Soc. Jpn. 70, 813–836.

Legates, D.R., Willmont, C., 1990a. Mean seasonal and spatial variability in gauge-corrected, global precipitation. Int. J. Climatol. 10, 111–127.

Legates, D.R., Willmont, C., 1990b. Mean seasonal and spatial variability in global surface air temperature. Theor. Appl. Climatol. 41, 11–21.

Lenters, J.D., Cook, K.H., 1997. On the origin of the Bolivian high and related circulation features of the South American climate. J. Atmos. Sci. 54, 656–677.

Liebmann, B., Marengo, J., 2001. Interannual variability of the rainy season and rainfall in the Brazilian Amazon Basin. J. Climate 14, 4308–4318.

Liebmann, B., Allured, D., 2005. Daily precipitation grids for South America. Bull. Am. Meteorol. Soc. 86, 1567–1570.

Liebmann, B., Kiladis, G., Marengo, J., Ambrizzi, T., Glick, J.D., 1999. Submonthly convective variability over South America and the South Atlantic Convergence Zone. J. Climate 11, 2898–2909.

Madden, R., Julian, P., 1994. A review of the intraseasonal oscillation in the Tropics. Mon. Weather Rev. 122, 814–837.

Mantua, N.J., Hare, S., Zhang, Y., Wallace, J.M., Francis, R.C., 1997. A Pacific interdecadal climate oscillation with impacts on salmon production. Bull. Am. Meteorol. Soc. 78, 1069–1079.

Marengo, J., 1992. Interannual variability of surface climate in the Amazon basin. Int. J. Climatol. 12, 853–863.

Marengo, J., 2004. Interdecadal and long-term rainfall variability in the Amazon basin. Theor. Appl. Climatol. 78, 79–96.

Marengo, J., Nobre, C., 2001. The Hydroclimatological framework in Amazonia. In: Richey, J., McClaine, M., Victoria, R. (Eds.), Biogeochemistry of Amazonia. Oxford Univ. Press, Oxford, pp. 17–42.

Marengo, J., Liebmann, B., Kousky, V.E., Filizola, N., Wainer, I.C., 2001. Onset and end of the rainy season in the Brazilian Amazon Basin. J. Climate 14, 833–852.

Marengo, J., Soares, W., Saulo, C., Nicolini, M., 2004. Climatology of the LLJ east of the Andes as derived from the NCEP reanalyses. J. Climate 17, 2261–2280.

Marengo, J., Nobre, C., Tomasella, J., Sampaio, G., Camargo, H., 2008. The drought of Amazonia in 2005. J. Climate 21, 495–516.

Marshall, G.J., 2003. Trends in the southern annular mode from observations and reanalyses. J. Climate 16, 4134–4143.

Masiokas, M., Villalba, R., Luckman, B., Le Quesne, C., Aravena, J.C., 2006. Snowpack variations in the Central Andes of Argentina and Chile, 1951–2005. Large-scale atmospheric influences and implications for water resources in the region. J. Climate 19, 6334–6352.

Mitchell, T.P., Wallace, J.M., 1992. The annual cycle in the equatorial convection and sea surface temperature. J. Climate 5, 1140–1156.

Mitchell, T.D., Jones, P.D., 2005. An improved method of constructing a database of monthly climate observations and associated high-resolution grids. Int. J. Climatol. 25, 693–712.

Montecinos, A., Aceituno, P., 2003. Seasonality of the ENSO-related rainfall variability in central Chile and associated circulation anomalies. J. Climate 16, 281–296.

Montecinos, A., Díaz, A., Aceituno, P., 2000. Seasonal diagnostic and predictability of rainfall in subtropical South America based on tropical Pacific SST. J. Climate 13, 746–758.

Moura, A.D., Shukla, J., 1981. On the dynamics of droughts in Northeast Brazil: observations, theory and numerical experiments with a general circulation model. J. Atmos. Sci. 38, 2653–2675.

Nakamura, H., Shimpo, A., 2004. Seasonal variations in the southern hemisphere storm tracks and jet streams as revealed in a reanalysis dataset. J. Climate 17, 1828–1844.

New, M., Hulme, M., Jones, P., 2000. Representing twentieth-century space-time climate variability. Part II: development of 1901–1996 monthly grids of terrestrial surface climate. J. Climate 13, 2217–2238.

Newman, M., Compo, G.P., Alexander, M.A., 2003. ENSO-forced variability of the Pacific Decadal Oscillation. J. Climate 16, 3853–3857.

Nobre, P., Shukla, J., 1996. Variations of sea surface temperature, wind stress and rainfall over the tropical Atlantic and South America. J. Climate 9, 2464–2479.

Nogues-Paegle, J., Mo, K.C., 1997. Alternating wet and dry conditions over South America during summer. Mon. Weather Rev. 125, 279–291.

Nogués-Paegle, J., Mo, K.C., 2002. Linkages between summer rainfall variability over South America and sea surface temperature anomalies. J. Climate 15, 1389–1407.

Nogués-Paegle, J., Byerle, L., Mo, K.C., 2000. Intraseasonal modulation of South American summer precipitation. Mon. Weather Rev. 128, 837–850.

Peterson, T., Vose, R., 1997. An overview of the global historical climatology network temperature database. Bull. Am. Meteorol. Soc. 78, 2837–2849.

Poveda, G., Jaramillo, A., Gil, M., Quiceno, N., Mantilla, R., 2001. Seasonally in ENSO-related precipitation, river discharges, soil moisture, and vegetation index in Colombia. Water Resour. Res. 37 (8), 2169–2178.

Quadrelli, R., Wallace, J.M., 2004. A simplified linear framework for interpreting patterns of northern hemisphere wintertime climate variability. J. Climate 17, 3728–3744.

Rao, V., de Lima, M.C., Franchito, S., 1993. Seasonal and interannual variations of rainfall over eastern northeast Brazil. J. Climate 6, 1754–1763.

Robertson, A.W., Mechoso, C.R., 2000. Interannual and interdecadal variability of the South Atlantic Convergence Zone. Mon. Weather Rev. 128, 2947–2957.

Ronchail, J., Gallaire, R., 2006. ENSO and rainfall along the Zongo valley (Bolivia) from the Altiplano to the Amazon basin. Int. J. Climatol. 26, 1223–1236.

Ronchail, J., Cochonneau, G., Molinier, M., Guyot, J., Goretti De Miranda, A., Guimarães, V., Oliveira, E., 2002. Interannual rainfall variability in the Amazon basin and sea-surface temperatures in the equatorial Pacific and the tropical Atlantic Oceans. Int. J. Climatol. 22, 1663–1686.

Ropelewski, C., Halpert, M., 1987. Global and regional scale precipitation patterns associated with the El Niño/Southern Oscillation. Mon. Weather Rev. 115, 1606–1626.

Rutllant, J., Fuenzalida, H., 1991. Synoptic aspects of the central Chile rainfall variability associated with the Southern Oscillation. Int. J. Climatol. 11, 63–76.

Rutllant, J., Fuenzalida, H., Aceituno, P., 2003. Climate dynamics along the arid northern coast of Chile: the 1997–1998 Dinámica del Clima de la Región de Antofagasta (DICLIMA) experiment. J. Geophys. Res. 108 (D17), 4538. doi:10.1029/2002JD003357.

Satyamurty, P., Nobre, C., Silva Dias, P.L., 1998. South America. In: Karoly, D.J., Vincent, D. (Eds.), Meteorology of the Southern Hemisphere (Monograph Series No. 27). Am. Meteor. Soc., Boston, USA, pp. 119–140.

Saulo, A.C., Nicolini, M., Chou, S.C., 2000. Model characterization of the South American low-level flow during the 1997–98 spring–summer season. Clim. Dyn. 16, 867–881.

Schneider, N., Cornuelle, B.D., 2005. The forcing of the Pacific Decadal Oscillation. J. Climate 18, 4355–4373.

Schwerdtfeger, W., Landsberg, H.E., 1976. Climate of Central and South America. World Survey of Climatology, vol. 12. Elsevier, Amsterdam.

Seluchi, M.E., Saulo, C., Nicolini, M., Satyamurty, P., 2003. The northwestern Argentinean Low: a study of two typical events. Mon. Weather Rev. 131, 2361–2378.

Silvestri, G.E., 2005. Comparison between winter precipitation in southeastern South America during each ENSO phase. Geophys. Res. Lett. 32, L05709. doi:10.1029/2004GL021749.

Please cite this article as: Garreaud, R.D., et al., Present-day South American climate, Paleogeogr. Palaeoclimatol. Palaeoecol. (2008), doi:10.1016/j.palaeo.2007.10.032

Silvestri, G.E., Vera, C.S., 2003. Antarctic Oscillation signal on precipitation anomalies over southeastern South America. Geophys. Res. Lett. 30 (21), 2115. doi:10.1029/2003GL018277.
Thompson, D.W.J., Wallace, J.M., 2000. Annular modes in the extratropical circulation. Part I: month-to-month variability. J. Climate 13, 1000–1016.
Thompson, D.W.J., Solomon, S., 2002. Interpretation of recent southern hemisphere climate change. Science 296, 895–899.
Trenberth, K.E., 1991. Storm tracks in the Southern Hemisphere. J. Atmos. Sci. 48, 2159–2178.
Uppala, S.M., et al., 2005. The ERA-40 re-analysis. Q. J. R. Meteorol. Soc. 131, 2961–3012.
van Loon, H., 1972. Temperature, pressure, wind, cloudiness and precipitation in the Southern Hemisphere. Meteorology of the Southern Hemisphere, Meteorological Monographs, N° 35. Amer. Meteor. Soc. 25–111.
Vera, C.S., Silvestri, G., Barros, V., Carril, A., 2004. Differences in El Niño response over the Southern Hemisphere. J. Climate 17, 1741–1753.
Vera, C., Higgins, W., Amador, J., Ambrizzi, T., Garreaud, R., Gochis, D., Gutzler, D., Lettenmaier, D., Marengo, J., Mechoso, C.R., Nogues-Paegle, J., Silva Diaz, P.L., Zhang, C., 2006. Towards a unified view of the American Monsoon System. J. Climate 19, 4977–5000.
Virji, H., 1981. A preliminary study of summertime tropospheric circulation patterns over South America estimated from cloud winds. Mon. Weather Rev. 109, 599–610.
Vuille, M., 1999. Atmospheric circulation over the Bolivian Altiplano during dry and wet periods and extreme phases of the Southern Oscillation. Int. J. Climatol. 19, 1579–1600.
Vuille, M., Keimig, F., 2004. Interannual variability of summertime convective cloudiness and precipitation in the central Andes derived from ISCCP-B3 data. J. Climate 17, 3334–3348.
Vuille, M., Bradley, R.S., Keimig, F., 2000a. Climate variability in the Andes of Ecuador and its relation to tropical Pacific and Atlantic sea surface temperature anomalies. J. Climate 13, 2520–2535.
Vuille, M., Bradley, R.S., Keimig, F., 2000b. Interannual climate variability in the Central Andes and its relation to tropical Pacific and Atlantic forcing. J. Geophys. Res. 105, 12,447–12,460.
Wang, X.L., Swail, V.R., Zwiers, F.W., 2006. Climatology and changes of extratropical cyclone activity: comparison of ERA-40 with NCEP/NCAR reanalysis for 1958–2001. J. Climate 19, 3145–3166.
Wolter, K., Timlin, M.S., 1998. Measuring the strength of ENSO events – how does 1997/98 rank? Weather 53, 315–324.
Wylen, P., Compagnucci, R., Caffera, R.M., 2000. Interannual and interdecadal variability in streamflow from the Argentine Andes. Phys. Geogr. 21, 452–465.
Xie, P., Arkin, P.A., 1997. Global precipitation: a 17-year monthly analysis based on gauge observations, satellite estimates, and numerical model outputs. Bull. Am. Metorol. Soc. 78, 2539–2558.
Zhou, J., Lau, K.M., 1998. Does a monsoon climate exist over South America? J. Climate 11, 1020–1040.

Please cite this article as: Garreaud, R.D., et al., Present-day South American climate, Paleogeogr. Palaeoclimatol. Palaeoecol. (2008), doi:10.1016/j.palaeo.2007.10.032